Fluvial Channel Size Determination with Indicator Variograms

Hong Guo and Clayton V. Deutsch

Geological models of fluvial reservoirs are often constructed with object based modeling techniques. This approach requires a specification of the distribution of channel sizes determined traditionally from core and well log data. The problem with this data is that it only shows the apparent thicknesses of the channel objects: sometimes the thicknesses are too small because the well intersects the channel at the edge and sometimes the thicknesses are too large because channels are stacked. This paper proposed a new approach to determine reasonable fluvial channel sizes with indicator variograms. The relationship between the channel geometry and the variogram is established. The relationship is verified with synthetic examples. The calculated indicator variogram range is shown to be insensitive to channel width and width/thickness ratio. Two real reservoir examples show how the approach works in practice.

Introduction

There are a variety of facies simulation methods for modeling petroleum reservoirs and other geological sites. These methods can be grouped into object-based and pixel-based techniques. Seifert & Jensen (2000) compare them when modelling a braided fluvial system. Object-based facies modeling performs well for situations where the geometry of the facies is relatively clear such as in many fluvial depositional environments. Object-based techniques proceed by placing selected facies objects within a background facies type. Object-based methods have been widely used and are documented in many papers including Damsleth *et al.* 1992; MacDonald *et al.* 1992; Alabert & Modot 1992; Deutsch & Wang 1996; Holden *et al.* 1998; Skorstad *et al.* 1999.

Fluvial depositional systems are complex (Miall 1984, 1996; Galloway & Hobday 1983). This paper focuses on modeling a well-defined channel geometry. The channel form will be filled with point bar sands, shale plugs and, possibly, other heterolithic facies. The internal distribution of facies and continuous properties such as porosity and permeability are modeled after the channel form geometry.

Modeling fluvial channel facies with object-based techniques requires a specification of the size of the channel objects. The parameters used to define geometrically a channel include the channel maximum thickness T (it will be denoted as the channel thickness in this paper), channel width W and the relative position b of the channel thickness. The cross section of an idealized channel is calculated as:

$$b = \begin{cases} \frac{1}{2}\left(1 - \frac{|C_v|}{C_v^l}\right) & C_v < 0 \\ \frac{1}{2}\left(1 + \frac{C_v}{C_v^r}\right) & C_v < 0 \\ \frac{1}{2} & C_v = 0 \end{cases} \qquad (1)$$

where C_v is the local curvature, C_v^l and C_v^r denote the maximum absolute value of C_v

Traditionally, well log and core data are used to determine the channel thicknesses. The channel width is often inferred from channel width/channel thickness ratios from analogue data or outcrop studies. Miall (1996, p. 329, fig. 10.21, p. 330, fig. 10.22) gives some plot references demonstrating the relationship between the channel depth and channel width. The main drawback of this traditional method is that the apparent thickness observed from well logs and core does not necessarily represent the true channel thickness. The apparent channel thicknesses are less than the true channel thicknesses if a well penetrates a channel object in its margin (Fig. 1, location A in well 1); in other cases, the apparent thicknesses can be larger than true thicknesses because of amalgamation of several channel objects (Fig. 1, location B in well 2). The difference between them can be up to 10 times. The case when the apparent channel thickness is equal to the true channel thickness is rarely encountered in practice.

The inconsistency between the apparent channel thickness determined by core or well data and the true channel thickness makes the resulting facies models inconsistent with the true channel distribution, which will continue influencing the following porosity modeling and permeability modeling. Also, the apparent thickness will mislead us to introduce some wrong vertical trends as well as give an improper reserve estimation. This paper introduces a new approach to calculate the channel thickness from the

well data. The theoretical link between the channel geometry and the indicator variogram is established. The indicator variogram is reliably calculated from limited well data, then the channel geometry can be inferred and used in object based modeling.

Indicator Variograms

Indicator variograms are used in geostatistics to measure spatial variability of indicator variables (Alabert 1987; Deutsch & Journel 1992; Journel & Gomez-Hernandez 1993) using the transitions between facies and not the facies themselves. Variograms are frequently used for quantitative analysis of spatial variation in lithology or facies (Journel & Huijbregts 1978; Jones & Ma 2001).

The indicator variable at location **u** is defined as:

$$\mathrm{i}(\mathbf{u};\mathrm{channel}) = \begin{cases} 1, if\ location\ \boldsymbol{u}\ in\ channel\ facies \\ 0, otherwise \end{cases} \quad (2)$$

At an unsampled location, the indicator random variable is denoted *I(**u**;k)*, where *k* is the facies index.

The indicator variogram for a lag separation vector **h** is defined as:

$$2\gamma_{\mathrm{I}}(\mathbf{h};\mathrm{k}) = \mathrm{E}\{[\mathrm{I}(\mathbf{u};\mathrm{k}) - \mathrm{I}(\mathbf{u}+\mathbf{h};\mathrm{k})]^2\} \quad (3)$$

Traditionally, indicator variograms are fitted empirically with a nested combination of mathematical functions such as the spherical, exponential, and Gaussian models (Christakos 1984; Deutsch & Journel 1992). The indicator variogram model used in this paper is a modified model based on geometric offsets (Pyrcz & Deutsch 2006). The nonstandardized indicator variograms for the object-based Boolean simulation (Deutsch & Journel 1998) in the next section are fitted using a variogram model as follows:

$$\gamma(\mathbf{h}) = \mathrm{p}_1\left(1 - \mathrm{p}_1{}^{\mathrm{Sph}(\mathbf{h})}\right) \quad (4)$$

Where, p_1 is the probability that the indicator at a point is 0 (i.e. the volume fraction outside the spheres). $\mathrm{Sph}(\mathbf{h})$ corresponds to the geometric offsets of a spherical object, that can be defined as:

$$\mathrm{Sph}(\mathbf{h}) = \frac{\mathrm{V}-\mathrm{V}_{\mathrm{ints}}}{\mathrm{V}} = \begin{cases} \frac{3}{2}\frac{\mathbf{h}}{\mathrm{a}} - \frac{1}{2}\left(\frac{\mathbf{h}}{\mathrm{a}}\right)^3, \mathbf{h} < \mathrm{a} \\ 1, \mathrm{otherwise} \end{cases} \quad (5)$$

Where, V is the volume of the spheres, and $\mathrm{V}_{\mathrm{ints}}$ is the volume of intersection. **h** is the separation lag, and a is the variogram range which is equal to 2R in this case.

The nonstandardized indicator variograms for the fluvial channel objects used in the next section (Deutsch & Tran 2002) are also fitted using a variogram model based on geometric offsets as follows:

$$\gamma(\mathrm{h}) = \mathrm{p}_1\left(1 - \mathrm{p}_1{}^{\mathrm{Chan(h)}}\right) \quad (6)$$

Where, p_1 is the probability that the indicator at a point is 1 (i.e. the volume fraction outside the channels). $\mathrm{Chan(h)}$ is a variogram function customed for channel, which can be defined as:

$$\mathrm{Chan(h)} = \frac{\mathrm{S}-\mathrm{S}_{\mathrm{ints}}}{\mathrm{S}} \quad (7)$$

Where, s is the area of the cross section of a channel, which is defined as (Deutsch & Wang 1996):

$$\mathrm{s} = \frac{4\times\mathrm{a}\times\mathrm{W}\times\mathrm{k}}{2\mathrm{k}^2+3\mathrm{k}+1} \quad (8)$$

Where, a is the channel thickness, which correspond to the indicator variogram range, and W is the channel width.

$$\mathrm{k} = \begin{cases} -\ln(2)/\ln(\mathrm{b}) & \text{if } \mathrm{b} \le 0.5 \\ -\ln(2)/\ln(1-\mathrm{b}) & \text{if } \mathrm{b} \ge 0.5 \end{cases} \quad (9)$$

$\mathrm{s}_{\mathrm{ints}}$ is the area of intersection in vertical direction shown in Fig. 4.

$$\mathrm{s}_{\mathrm{ints}} = \frac{4\cdot(\mathrm{a}-\mathrm{h})\times\mathrm{w}_{\mathrm{i}}\times\mathrm{k}}{2\mathrm{k}^2+3\mathrm{k}+1} \quad (10)$$

Where w_{i} is the width of the intersection area indicated by the shaded region, and h is the separation lag in vertical direction. The equation for the depth of the channel base below the channel top when b≤0.5 (maximum thickness closer to the left bank) is:

$$\mathrm{d(w)} = 4\times\mathrm{a}\times\left(\frac{\mathrm{w}}{\mathrm{W}}\right)^{-\ln(2)/\ln(\mathrm{b})}\times\left[1-\left(\frac{\mathrm{w}}{\mathrm{W}}\right)^{-\ln(2)/\ln(\mathrm{b})}\right] \quad (11)$$

When b>0.5,

$$\mathrm{d(w)} = 4\times\mathrm{a}\times\left(1-\frac{\mathrm{w}}{\mathrm{W}}\right)^{-\ln(2)/\ln(1-\mathrm{b})}\times\left[1-\left(1-\frac{\mathrm{w}}{\mathrm{W}}\right)^{-\ln(2)/\ln(1-\mathrm{b})}\right] \quad (12)$$

$\mathrm{w} \in [0, \mathrm{W}]$

Two width position w_{r} and w_{l} corresponding to d(w)=h can be derived from (11) or (12), and then w_{i} can be calculated as:

$$w_i = w_r - w_l \quad (13)$$

The geometric offset based model for the indicator variogram presented above not only fits the indicator variogram, but also can be used to derive the indicator variogram range.

Methods to Calculate the Range of the Indicator Variogram

Traditionally, the distance where the standardized indicator variogram reaches 1 is taken as the variogram range. This method is very easy to implement, however, variograms may not reach the sill or they may oscillate near the sill, see Fig. 2 for example; this makes it difficult to simply determine the channel thickness through the indicator variogram range. This method is compared with alternatives.

A new method is presented in this paper to derive the variogram range using a linear combination of estimates from each lag. The indicator variogram is the function of object proportion and size (range) as (4) and (6).

We can get a series of indicator variogram range a_i knowing object proportion and the indicator variogram values $\gamma(h_i)$ in each lag h_i through reverse educing from the variogram expression. The indicator variogram is quite stable and close to the theoretical indicator variogram at small distances (see Fig. 5). So, we can calculate the variogram range using a linear combination of estimates from each lag just within a relatively small distance.

$$a^* = \sum_{i=1}^{n_h} \omega_i \times a_i \quad (14)$$

Where ω_i is the weights assigned to the calculated variogram range a_i in each lag. Within a certain distance, smaller the lag is, more stable the experimental indicator variogram shows, so we set the weight ω_i to be in inverse ratio to the lag hi.

Randomly choosing some sample wells from a synthetic fluvial reservoir model, the range of the indicator variogram can be calculated using these sample well data, and the calculated range will be different under different well choices. For example, we want to use 10 wells to calculate the indicator variogram range, and the results couldn't be the same if we choose these 10 wells at different locations. A histogram of the range for different well choices can reflect the variance between them. We randomly selected 5, 10, 15, 20, and 30 wells from a synthetic fluvial reservoir. For different wells choices, we set up the histogram of ranges calculated using two different range determining methods (see Fig. 3). It can be seen that the mean range is closer to the true thickness and the standard deviation becomes less when the number of wells increases.

As shown in Fig. 3, the indicator variogram range determined using the traditional method has a larger variance than that derived from new method. The proposed method is straightforward to implement and it will be used to determine the indicator variogram range in subsequent sections.

Link Between Object Size and Indicator Variograms in Synthetic Examples

For randomly placed objects created by the Bombing model (Hall 1988) using the program ellipsim (Deutsch & Journel 1998), the indicator variogram range is equal to the real object size. The indicator variogram range is not sensitive to the proportion of objects; the proportion of objects just alters the shape of the indicator variogram. Although there is more amalgamation of objects when the global object proportion increases, the indicator variogram range represents the real object size. This feature of indicator variograms is also mentioned by Leuangthong *et al.* (2008).

Four object-based fluvial channel models were generated on a 500m×500m×8m domain using the program fluvsim (Deutsch & Tran 2002). In this model, only two facies are considered: the channel fill facies and the background facies. The channels have a width of 50m and a thickness of 1m with a sinuosity departure of 30m. Vertical indicator variograms for the channel objects with different global proportion are given in Fig. 4. The indicator variogram range reflects the real thickness of the channel objects even if amalgamation of channel objects exists. The indicator variograms can be fit using geometric offsets based channel variogram model with the range of 1m.

The indicator variogram range is closely related to the real object size. This approach would be complicated by a distribution of channel sizes. In this case, the calculated channel size would be an effective channel size. The indicator variograms shown above were calculated with the entire grid of data. In practice, there are only a few wells and the calculated variogram would not be as stable. This is

illustrated below. Some synthetic wells are chosen randomly from the above synthetic fluvial channel model to calculate the indicator variogram range. The standardized indicator variograms calculated using 10 randomly selected wells are shown in Fig. 2. 10 curves denote 10 different selected wells. Note that the indicator variogram range changes with different wells, and in some cases, the indicator variogram range is difficult to determine because of the variability of indicator variogram close to the sill. The new method proposed above to determine the indicator variogram range works well.

The fluvial channel objects we considered have the same size, however, in practice, there may be channels of different sizes. In this case, an effective size is calculated. Different triangular channel size distributions are considered in fluvial simulation to check the effective object thickness determined from the indicator variogram ranges. No matter the value of channel thickness distribution and sinuosity departure change, the effective thickness derived from indicator variogram remains close to the mean of the input channel thickness distribution, and the effective thickness decreases when the thickness distribution becomes narrow, which means that thick channels affect the effective value more than thin channels. In practice, the range of variation in channel size must be chosen from geological knowledge.

Application of the Proposed Approach to Real Well Data

Determining the object size using indicator variogram has proven robust in the synthetic examples shown above; however, it is interesting to see how the method works with real data. A set of core data including fluvial channel facies from a North Sea Reservoir (Journel *et al.* 1998; Yao 2002) is considered. The histogram of apparent thicknesses can be seen in Fig. 5. The apparent thicknesses cover a range from 0.1m to 11.7m with the mean of 2.42m. Fig. 6 shows the calculated vertical indicator variogram for channel facies, which gives a good example of the application of the proposed approach. A set of core data in 15 wells are considered in this case. The indicator variogram for long distances shows vertical cyclicity, and the indicator variogram for short distances shows the indicator variogram in detail. The calculated variogram range is 3.5m which can be used as an effective thickness for channel objects and the indicator variogram can be well fit using the channel variogram model (6).

Another application example is shown in Fig. 7, which shows the calculated channel facies indicator variogram for a set of core data from the McMurray formation in Northern Alberta. The histogram of apparent thicknesses looks like Fig. 8. There is a large range of apparent thicknesses from 0.5m to 35m. The calculated indicator variogram range of 13.2m, which is large different to the mean apparent thickness of 5.1m, can be used as an effective channel thickness, and the indicator variogram can be fit using the channel variogram model with a nugget effect. Determining an effective thickness using the indicator variogram range appears to be a reasonable approach when applied to these two sets of real data. The generation of channels is a complicated process. The shape and size may have been modified by erosion or structural deformation. The shape may not be the idealized shape shown above. There may be thin intervals of mud or other facies that make the channels appear discontinuous. This is illustrated in the variogram shown in Fig. 7. There may be trends and other anisotropy that confound the variogram. Figure 9 is an example for the indicator variogram calculated using real data with the existence of zonal anisotropy. These factors will make the indicator variogram depart from the expected theoretical shape. The results and interpretations must be checked carefully.

Discussion and Conclusion

A new method is proposed in this paper to determine the effective channel object size using the indicator variogram range and it has been proven theoretically valid using synthetic fluvial reservoir models. An important advantage of this method is that the channel thickness calculated from the vertical indicator variograms is not sensitive to the channel width or width/thickness ratio. The geometric offset based variogram model is introduced to fit the indicator variogram for the fluvial model. The geometry of the channels is assumed. Two methods to determine the indicator variogram range are presented. Their merits and shortcomings are listed in this paper. The new method of using the linear combination of estimates in each lag within a stable distance as the variogram range is our preferable method to specify the effective thickness for single-sized channel objects and mix-sized channel objects. Two application examples show the validity of the recommended method in this paper to determine the effective thickness using indicator variogram range; however, there are still some challenges for us to use this

approach to determine the effective channel object size in practice. Lack of knowledge for the channel objects, complexity of generation and development of channel objects, and the existence of geometric anisotropy and zonal anisotropy in some interested domain will result in some difficulty to the practical application of this method. Taking one with another, specifying effective thickness for fluvial channel objects using the indicator variogram followed by inferring the channel width from channel width/ thickness ratio through geological studies is a valid and flexible method to determine the fluvial channel object size. Actually, it can also determine an effective object size for any other kinds of objects if we can give a customized geometric offset based variogram model for them.

Reference

Alabert, F. 1987. *Stochastic imaging of spatial distributions using hard and soft information.* M. Sc Thesis, Stanford University.

Alabert, F. G. & Modot, V. 1992. *Stochastic models of reservoir heterogeneity: Impact on connectivity and average permeabilities.* Paper SPE 24893 presented at the 1992 SPE Annual Technical Conference & Exhibition, Washington, DC, Oct. 4–7, 355–370.

Christakos, G. 1984. On the problem of permissible covariance and variogram models. *Water Resources Research*, **20**, 251-205.

Damsleth, E., Tjølsen, C. B., Omre, H. & Haldorsen, H. H. 1992. A two-stage stochastic model applied to a North Sea Reservoir. *Journal of Petroleum Technology*, **44**, 402–408.

Deutsch, C. V. & Journel, A. G. 1992. GSLIB: Geostatistical software library and user's guide. Oxford University Press, New York.

Deutsch, C. V. & Wang, L. 1996. Hierarchical object-based stochastic modeling of fluvial reservoirs. *Mathematical Geology*, **28**, 857-880.

Deutsch, C. V. & Journel, A. G. 1998. GSLIB: geostatistical software library and user's guide 2nd ed. Oxford University Press, New York.

Deutsch, C. V. & Tran, T. T. 2002. FLUVSIM: A Program for Object-Based Stochastic Modeling of Fluvial Depositional Systems. *Computers & Geosciences*, **28**, 525-535.

Galloway, W. E. & Hobday, D. K. 1983. Terrigenous clastic depositional systems: applications to petroleum, coal, and uranium exploration. Springer-Verlag, New York.

Hall P. 1988. Introduction to the theory of coverage processes. John Wiley & Sons Inc., New York.

Holden, L., Hauge, R., Skare, Ø. & Skorstad, A. 1998. Modeling of fluvial reservoirs with object models. *Mathematical Geology*, **30**, 473–496.

Journel, A. G. & Huijbregts, Ch. J. 1978. Mining geostatistics. Academic Press, New York.

Journel, A. G. & Gomez-Hernandez, J. J. 1993. Stochastic imaging of the Wilmington clastic sequence. *SPE Formation Evaluation*, **8**, 33-40.

Journel, A. G., Gundeso, R., Gringarten, E. & Yao, T. 1998. Stochastic modelling of a fluvial reservoir: A comparative review of algorithms. *Journal of Petroleum Science & Engineering*, **21**, 95–121.

Jones, T. A. & Ma, Y. Z. 2001. Geologic characteristics of hole-effect variograms calculated from lithology-indicator variables. *Mathematical Geology*, **33**, 615–629.

Leuangthong, Oy., Khan, K. Daniel. & Deutsch, C.V. 2008. Solved problems in geostatistics. John Wiley & Sons, Inc., Hoboken, New Jersey.

MacDonald, A. C., Høye, T. H., Lowry, P., Jacobsen, T., Aasen, J. O. & Grindheim, A. O. 1992. Stochastic flow unit modeling of a North Sea coastal-deltaic reservoir. *First Break*, **10**, 124–133.

Miall, A. D. 1984. Variations in fluvial style in the Lower Cenozoic synorogenic sediments of the Canadian Arctic Islands. *Sedimentary Geology*, **38**, 499-523.

Miall, A. D. 1996. The geology of fluvial deposits: sedimentary facies, basin analysis and petroleum geology. Springer-Verlag, Berlin, New York.

Pyrcz, M. J. & Deutsch, C. V. 2006. Semivariogram models based on geometric offsets. *Mathematical Geology*, **38**, 475-488.

Seifert, D. & Jensen, J. L. 2000. Object and pixel-based reservoir modeling of a braided fluvial reservoir. *Mathematical Geology*, **32**, 581-603.

Skorstad, A., Hauge, R. &Holden, L. 1999. Well conditioning in a fluvial reservoir model. *Mathematical Geology*, **31**, 857-872.

Yao,T. 2002. Integrating seismic data for lithofacies modeling: a comparison of sequential indicator simulation algorithms. *Mathematical Geology*, **34**, 387-403.

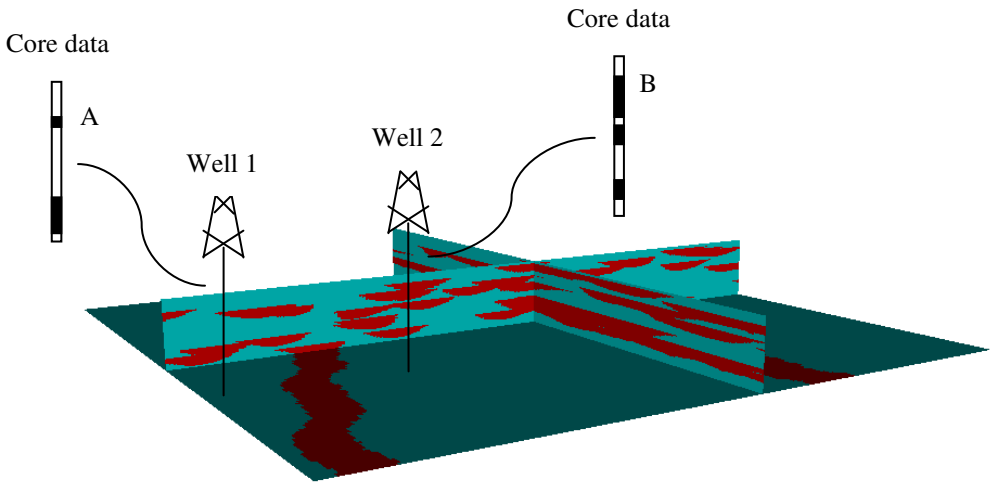

Figure 1. Illustration showing that the apparent thickness is not necessarily equal to the true thickness. Position A in Well 1 shows the case when apparent thickness < true thickness; Position B in Well 2 shows the case when apparent thickness > true thickness.

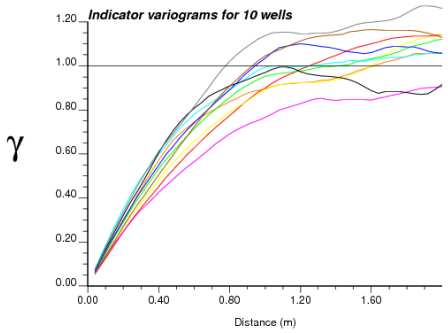

Figure 2. Indicator variograms for 10 sets of randomly selected sets of wells from fluvsim simulation in a 500m×500m domain.

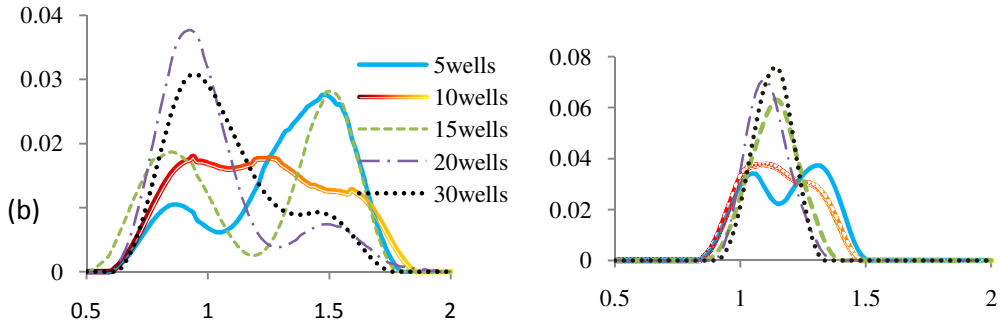

Figure 3. Histograms for variogram range estimates using 5, 10, 15, 20 and 30 wells. (a) variogram ranges are determined using the distance where the standardized variogram reaches the sill. (b) variogram ranges determined using the linear combination of estimates from each lag.

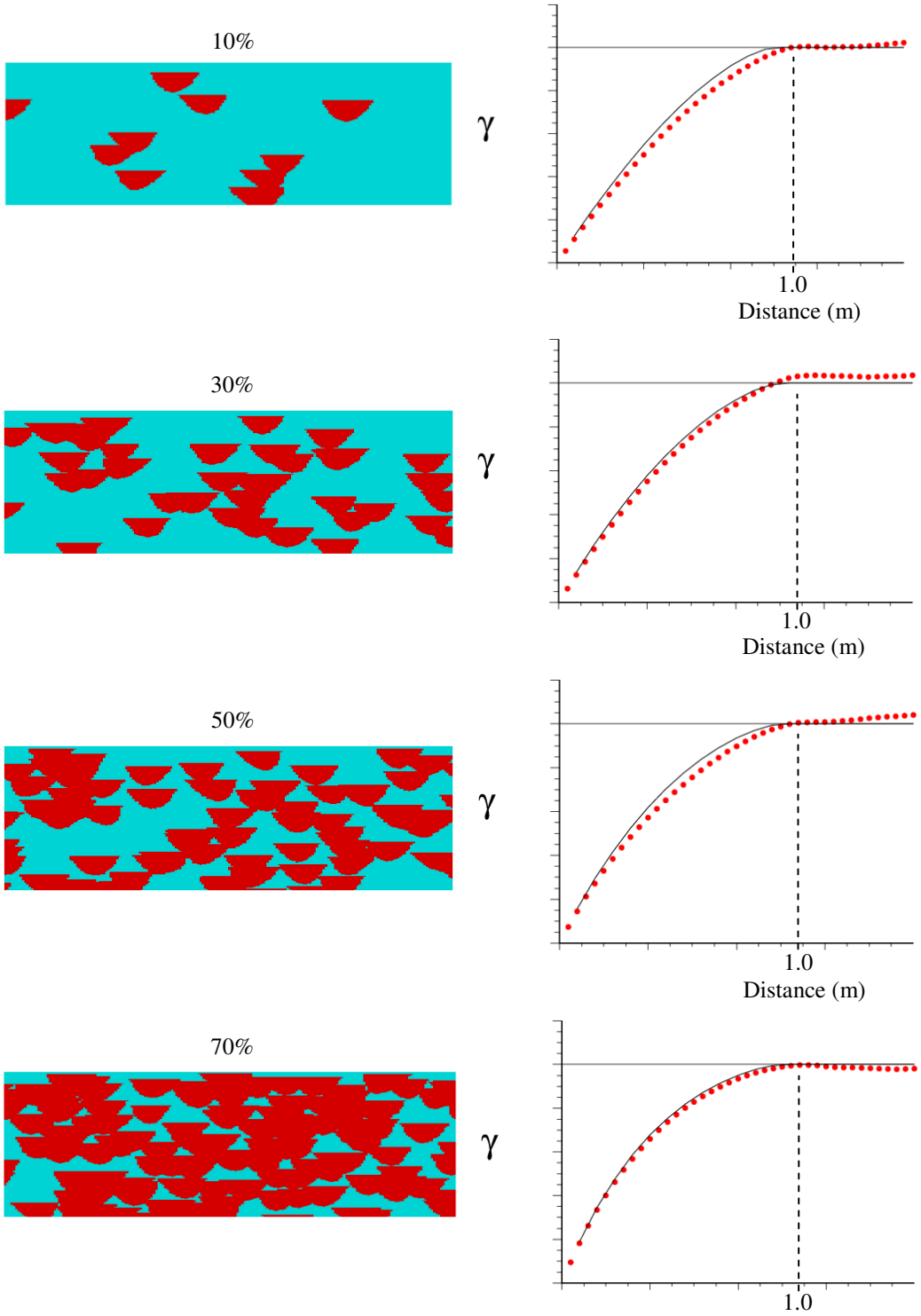

Figure 4. Vertical indicator variograms for the channel objects with proportions of 10%, 30%, 50%, and 70%from top to bottom.

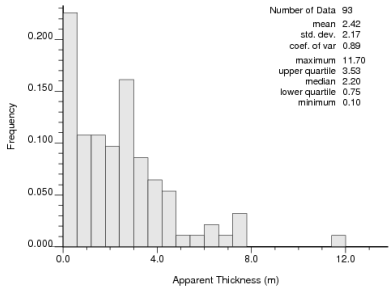

Figure 5. Histogram of the apparent channel thicknesses for a set of core data including fluvial channel facies from a North Sea Reservoir.

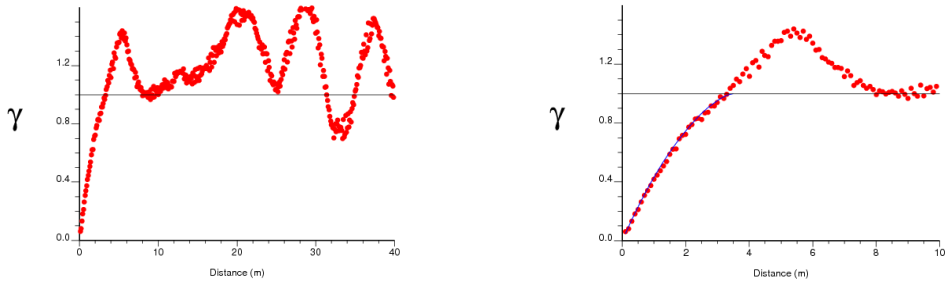

Figure 6. Vertical indicator variogram for the channel objects in North Sea Reservoir.

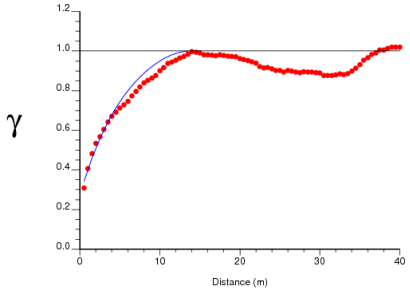

Figure 7. The indicator variogram for channel objects in McMurray formation. There are 100 densely distributed wells available, and the channel object proportion is 68%.

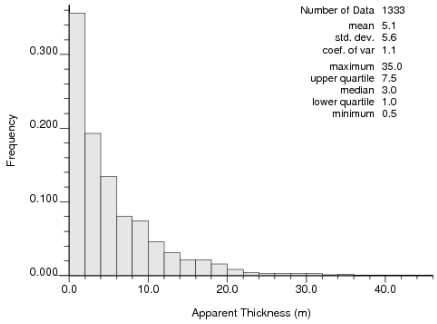

Figure 8. The histogram of apparent channel thicknesses for a set of core data including fluvial channel facies from McMurray Formation.

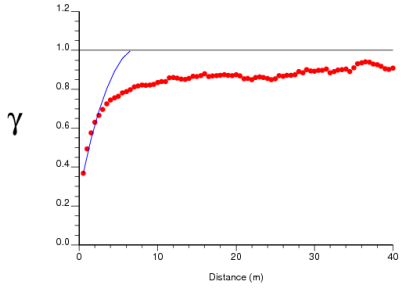

Figure 9. An example for the indicator variogram calculated using real data with zonal anisotropy.